MITSUBISHI ELECTRIC RESEARCH LABORATORIES
http://www.merl.com

Molecular Signaling Design Exploiting Cyclostationary Drift-Diffusion Fluid

Koike-Akino, T.; Suzuki, J.; Orlik, P.V.

TR2017-178 December 2017

Abstract

This paper investigates a method to improve performance of diffusive molecular communications between biologically-enabled nanomachines in in-vivo aqueous environment. The proposed method exploits periodic flow, e.g., induced by repeated heart pumping. We make an analysis of channel impulse response (CIR) for such drift-diffusion fluid systems. In order to take the cyclic CIR into account, the proposed method optimizes the release timing and size of information molecules so that highest equalization gain can be achieved. We reveal that error rate performance can be significantly improved with adaptive molecule loading by taking care of the cyclic CIR.

IEEE Global Communications Conference (GLOBECOM)

Molecular Signaling Design Exploiting Cyclostationary Drift-Diffusion Fluid

Toshiaki Koike-Akino*, Junichi Suzuki†, and Philip V. Orlik*
*Mitsubishi Electric Research Laboratories (MERL), 201 Broadway, Cambridge, MA 02139, USA
†Department of Computer Science, University of Massachusetts, Boston, Boston, MA 02125, USA
Email: {koike, porlik}@merl.com, jxs@cs.umb.edu

***Abstract*—This paper investigates a method to improve performance of diffusive molecular communications between biologically-enabled nanomachines in *in-vivo* aqueous environment. The proposed method exploits periodic flow, e.g., induced by repeated heart pumping. We make an analysis of channel impulse response (CIR) for such drift-diffusion fluid systems. In order to take the cyclic CIR into account, the proposed method optimizes the release timing and size of information molecules so that highest equalization gain can be achieved. We reveal that error rate performance can be significantly improved with adaptive molecule loading by taking care of the cyclic CIR.**

I. Introduction

Thanks to recent advancement on nano-scale bio-chemical engineering [1–3], molecular communications network [4–7] has emerged as a new paradigm to connect biologically-enabled nanomachines in the intrabody environment. The bio-machines are small-scale devices (nano-to-micro meter order) that are capable of sensing, actuating, computing, and exchanging data by means of information molecules. Molecular communications are expected to enable various biomedical and healthcare applications such as nanoscale lab-on-a-chip, in-situ physiological sensing, targeted drug delivery, artificial morphogenesis, and neural signal transduction [5–9].

It is known that molecular communications are inherently unreliable due to stochastic molecular propagation, molecule-to-molecule collisions, chemical degradation, and environmental noise. Accordingly, the molecular channels experience extremely long latency, large jitters, high erasure rate, and low capacity [10–13]. To deal with the unreliable molecular channels, several error control schemes have been investigated including feedback-based rate control [14–16], automatic repeat request [17, 18], and forward error correction [19–23]. In addition, various studies on molecular channel modeling [24–28, 30] revealed that we need to deal with a severe inter-symbol interference (ISI) caused by a long channel memory due to molecule diffusion. Hence, a typical receiver employs a communication distance estimation [31, 32], channel impulse response (CIR) acquisition [33], and ISI channel equalization [34–36].

In this paper, we investigate a transmitter design to enhance the equalization gain in a fluid environment having a periodic flow. This is motivated by the fact that biological behaviors such as heart pumping are often cyclic. For example, cardiac cycle in human body leads to periodic dynamics of blood flow [38]. Although molecular communications in the presence of constant flow have been studied in literature [34], there exist few studies analyzing the impact of periodic flow to the best of authors' knowledge. Since the expected CIR becomes cyclic, the error rate performance will be highly dependent on the molecule release timing. We show that a significant performance improvement may be achieved by adaptive control of molecular transmission to exploit the periodic channel memory.

The key contributions of this paper are summarized below.

- **Cyclic CIR analysis**: We analyze the impact of periodic flow on the channel memory for drift-diffusion molecular communications.
- **Release timing and particle size design**: To exploit the cyclic CIR, we optimize release timing at which the lowest error rate is achieved in a cycle for different particle sizes.
- **Adaptive molecule loading**: As an efficient resource assignment, we also propose an adaptive allocation of information molecules across a cycle to compensate for poor equalization performance at bad timing.

Notations: Throughout the paper, boldface lowercase letters denote column vectors. An operator $[\cdot]^{\mathrm{T}}$ denotes transpose, $\mathbb{E}[\cdot]$ represents the expectation, and $\mathsf{Pois}(\lambda)$ is a Poisson distribution with a mean of λ.

II. Molecular Communications System

Fig. 1 shows the molecular communications system under consideration, where a number of molecules are released from a transmitter (Tx) bio-nanomachine to a receiver (Rx) bio-nanomachine over *in-vivo* aqueous environment. The released molecules are propagated by stochastic diffusion process, i.e., Brownian motion. In addition to the diffusion, we consider drift flow, e.g., induced by heart pumping. We consider a tube-like transport such as vein blood vessel, whose diameter is about $5\,\mathrm{mm}$, which is relatively larger than the communication distance $x_0 \approx 300\,\mu\mathrm{m}$. For simplicity, we consider the communication distance does not change across the time, assuming that the Tx and Rx nanomachines are stabilized by membrane fixation.

A. Drift-Diffusion Molecular Propagation

In bio-physics [39], molecules propagated in fluid follow the stochastic differential equation:

$$\mathrm{d}x = \mu F(t)\mathrm{d}t + \sqrt{2D}\mathrm{d}w, \tag{1}$$

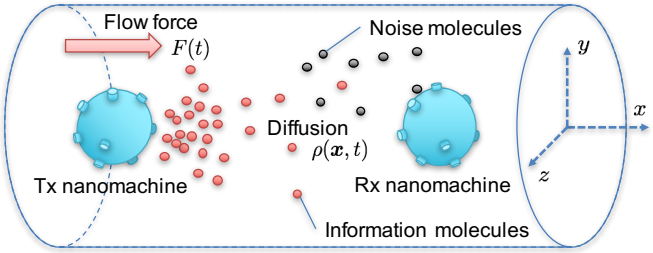

Fig. 1. Molecular communications system in drift-diffusion fluid environment.

where x is the location of molecule, μ is the mobility of the molecule in the fluid, $F(t)$ is time-varying external force in fluid, D is the diffusion coefficient, and $\mathrm{d}w$ denotes the Wiener process. The mobility is a function of viscosity η of environment ($\eta \simeq 10^{-3}$ kg/m/s for aqueous environment) and the effective radius R of molecules [39] as follows:

$$\mu = \frac{1}{6\pi\eta R}, \tag{2}$$

and the diffusion coefficient D is a function of the mobility μ according to the Einstein relation:

$$D = \mu k_{\mathrm{B}} T_0, \tag{3}$$

where $k_{\mathrm{B}} = 1.38 \times 10^{-23}$ J/K is the Boltzmann constant, and T_0 is the temperature in Kelvin.

The Fokker–Planck equation [41] for (1) provides the following drift-diffusion equation for the probability density function (PDF) $\rho(x,t)$ of the molecule distribution:

$$\frac{\partial \rho(x,t)}{\partial t} = -\mu F(t) \frac{\partial \rho(x,t)}{\partial x} + 2D \frac{\partial^2 \rho(x,t)}{\partial x^2}. \tag{4}$$

Supposed that the environment is unbounded (i.e., tube diameter is sufficiently larger than the communication distance) and the initial distribution released from the Tx nanomachine is Dirac's delta impulse assuming a point source, its solution is expressed as a Gaussian profile as follows:

$$\rho(x,t) = \frac{1}{\sqrt{4\pi D t}} \exp\left(-\frac{\big(x - m(t)\big)^2}{4Dt} \right), \tag{5}$$

where $m(t)$ is the mean of molecule location, which is derived by Itô's calculus [41] for (1) as follows:

$$m(t) = \mathbb{E}[x] = \int_0^t \mu F(\tau) \mathrm{d}\tau. \tag{6}$$

Note that the PDF in (5) is readily generalized to three-dimensional diffusion.

For the case when the information molecule can degrade via chemical reaction e.g., with enzymes, the concentration is also exponentially decaying over time. Specifically, the concentration $C(\boldsymbol{x},t)$ of the released molecules from the Tx nanomachine is modeled as follows [34]:

$$C(\boldsymbol{x},t) = \frac{N_{\mathrm{tx}}}{(4\pi D t)^{3/2}} \exp\left(-\kappa t - \frac{\big\|\boldsymbol{x} - \boldsymbol{m}(t)\big\|^2}{4Dt} \right), \tag{7}$$

where N_{tx} is the number of released molecules from Tx, κ is the degradation rate with a unit of s^{-1}, $\boldsymbol{x} = [x,y,z]^{\mathrm{T}}$ is the three-dimensional coordinate of the location, and $\boldsymbol{m}(t) = [m(t),0,0]^{\mathrm{T}}$ is the expected molecular location. Since we consider the tube-like transport with one-dimensional flow in Fig. 1, we focus on one-dimension diffusion throughput the paper. Nevertheless, our analysis is applicable to three-dimensional diffusion with a minor modification.

B. Cyclic Flow Environment

In [34], Noel et al. investigated optimal and sub-optimal receiver designs based on maximum-likelihood sequence detection (MLSD) and weighted-sum detection (WSD) for diffusive molecular communications in the presence of constant flow, i.e., $F(t) = F_0$ for all t. In this paper, we study transmitter design in the presence of periodic flow, i.e., $F(t) = F(t+T)$ with a certain duration of period T. This is motivated by the fact that biological functionalities are often cyclic. For example, a period of heart pumping is relatively stable around $T \simeq 1$ s. To the best of our knowledge, this is the first study investigating molecular communications in a time-varying flow fluid environment. We will show the potential improvement of transmission performance by exploiting the periodic channels.

In order to obtain useful insights in molecular transmissions under such cyclic drift-diffusion fluids, this paper considers a simplified case having sinusoidal flow force as follows:

$$F(t) = F_0 \cos^2(\pi t/T + \beta/2), \tag{8}$$

where F_0 and β denote the peak force and initial phase, respectively. In the presence of such sinusoidal force, the peak concentration is shifted at

$$m(t) = \frac{\mu F_0 t}{2} + \frac{\mu F_0}{4\pi/T}\Big(\sin(2\pi t/T + \beta) - \sin(\beta)\Big). \tag{9}$$

The first term comes from an averaged constant flow force $F_0/2$, while the rest of the terms are based on the contribution of time-varying sinusoidal force. The study for more realistic flow waveforms [38] will be left as a future work.

Fig. 2 shows the impact of particle size $R \in \{0.5, 1.0\}$ nm on the mean location $m(t)$ of molecular concentrations released from the Tx nanomachine at $t = 0$, $x = 0$, and initial phase of $\beta \in \{0, \pi/2, \pi\}$ rad. Here, we consider a peak force F_0 according to a typical peak blood pressure of 100 mmHg, i.e., $F_0 = \pi R^2 \cdot 13.3$ kN, where πR^2 comes from a total area of spherical particle of radius R. Although larger molecules have lower mobility (also diffusion coefficient) in general as in (2), a product of mobility μ and force F_0 can be increased given a certain pressure (i.e., force per unit area). In Fig. 3, we also illustrate several example snapshots of PDF evolution $\rho(x,t)$ over time at $t \in \{0.01, 0.02, 0.03\}$ s in the presence of sinusoidal flows. As shown in those figures, the molecular distribution is highly dependent on the initial phase β as well as the particle size R because of the specific characteristics in its mean and variance of the shifted Gaussian PDF $\rho(x,t)$.

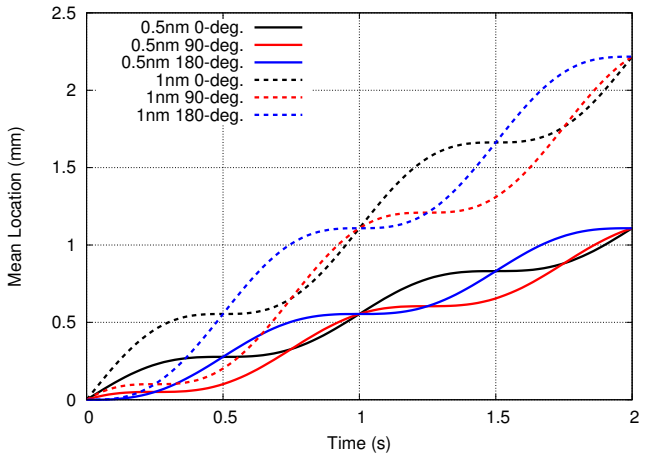

Fig. 2. Mean location $m(t)$ for particle sizes $R = \{0.5, 1.0\}$ nm with initial phases $\beta \in \{0, \pi/2, \pi\}$.

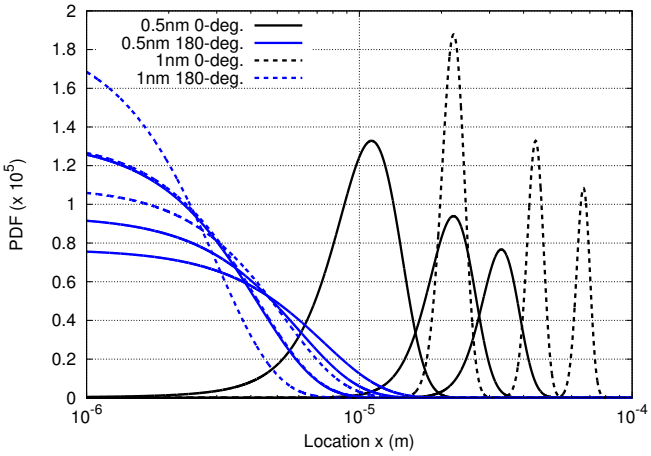

Fig. 3. Molecular PDF $\rho(x, t)$ for particle sizes $R = \{0.5, 1.0\}$ nm with initial phase $\beta \in \{0, \pi\}$ at time instance $t \in \{0.01, 0.02, 0.03\}$ s.

C. Channel Impulse Response (CIR)

The CIR for diffusive molecular communications has been intensively investigated in literature [13, 27, 30, 32–35, 40]. Assuming a transparent receiver [35], the expected number of arrival molecules at the Rx is obtained as

$$\bar{c}(t) = \int_{\boldsymbol{x} \in \mathbb{V}_{\rm rx}} C(\boldsymbol{x}, t) \mathrm{d}\boldsymbol{x}, \tag{10}$$

where $\mathbb{V}_{\rm rx}$ is the volume of the Rx nanomachine. For example, when a membrane-type Rx nanomachine of thickness $2R_{\rm rx}$ is located at x_0 for 1D Gaussian profile $\rho(x, t)$ in (5), the expected number of molecules is expressed by the error function $\mathrm{erf}(\cdot)$ as follows [37]:

$$\bar{c}(t) = \frac{N_{\rm tx}}{2} \left(\mathrm{erf}\left(\tfrac{x_0 + R_{\rm rx} - m(t)}{\sqrt{4Dt}} \right) - \mathrm{erf}\left(\tfrac{x_0 - R_{\rm rx} - m(t)}{\sqrt{4Dt}} \right) \right). \tag{11}$$

Note that the mean location $m(t)$ is given in (9) for sinusoidal flows.

Due to a Gaussian profile having long tail, the diffusive channels typically cause a severe ISI [13, 33–35, 40] unless the symbol interval $T_{\rm s}$ is chosen sufficiently large such that the CIR decays to a negligible level within one symbol interval. Because a long symbol interval will seriously limit the transmission rate of the communication system, we shall deal with ISI in practice by employing equalization techniques. The ISI channels in the molecular communications system can be modeled as follows [33]:

$$r[k] = \sum_{l=1}^{L} c_l[k] s[k - l + 1] + c_0[k] \triangleq \boldsymbol{c}^{\rm T}[k] \boldsymbol{s}[k], \tag{12}$$

where $r[k]$ is the number of molecules detected at the Rx in symbol instance $t = kT_{\rm s}$, L is the number of memory taps of the channel, $c_l[k]$ is the number of molecules observed at the Rx in symbol interval k contributed from the past molecule release from the Tx in symbol interval $k - l + 1$, and $s[k] \in \{0, 1\}$ denotes the on-off keying (OOK) concentration-modulated symbols [40]. Here, $c_0[k]$ is the number of external noise molecules detected by the Rx in symbol interval k but not released by the Tx nanomachine. We let $\boldsymbol{c}[k] \triangleq \big[c_0[k], c_1[k], c_2[k], \ldots, c_L[k]\big]^{\rm T}$ and $\boldsymbol{s}[k] \triangleq \big[1, s[k], s[k-1], \ldots, s[k-L+1]\big]^{\rm T}$ be stacked CIR (including noise) and transmission sequence at symbol instance k, respectively. According to literature [13, 27, 30, 32–35, 40], $c_l[k]$ is well modeled by a Poisson random variable (RV) with a mean of $\lambda_l[k] = \bar{c}((k - l)T_{\rm s})$, i.e., $c_l[k] \sim \mathsf{Pois}(\lambda_l[k])$. Noise molecules for $c_0[k]$ may originate from interfering sources employing the same type of molecule. Hence, $c_0[k]$ can also be modeled as a Poisson RV: $c_0[k] \sim \mathsf{Pois}(\lambda_0[k])$ with a mean of $\lambda_0[k]$.

Fig. 4 depicts examples of CIR (a.k.a. delay profile) $\bar{c}(t)$ normalized by $N_{\rm tx}$, i.e., arrival probability, at a communication distance of $x_0 = 300\,\mu$m. One can see that the CIR may have longer memory at some conditions, e.g., when released at the initial phase of $\beta = 0$ for a particle size of $R = 1.0$ nm. Fig. 5 shows the detailed impact of initial phase β on the delay profile for $R = 0.3$ nm. We observe that the delay profile highly depends on the release timing in the time-varying flow. In this paper, we exploit such a cyclic CIR to design the molecular transmission. In particular, short delay may not always be favorable since higher diversity gain may be potentially achieved by intentionally creating longer delay.

III. Molecular Signaling Design

In this section, we discuss a potential performance improvement by exploiting the cyclic CIR for molecular communications under drift-diffusion fluid environment with periodic flow. Unless otherwise stated, we assume a peak flow force corresponding to 133 Pa ($\pi R^2 \cdot 13.3$ kN) at a temperature of $T_0 = 35\,^\circ$C. The Tx nanomachine emits impulses of $N_{\rm tx} = 300$ molecules using OOK concentration modulation at a symbol interval of $T_{\rm s} = 10$ ms. When degradation is considered, we use $\kappa = 10$ /s. The radius of the information molecule is $R = 0.3$ nm, corresponding to a mobility of $\mu = 1.77 \times 10^{11}$ s/kg and a diffusion coefficient of $D = 7.52 \times 10^{-10}$ m^2/s according to (2) and (3). The Rx nanomachine with

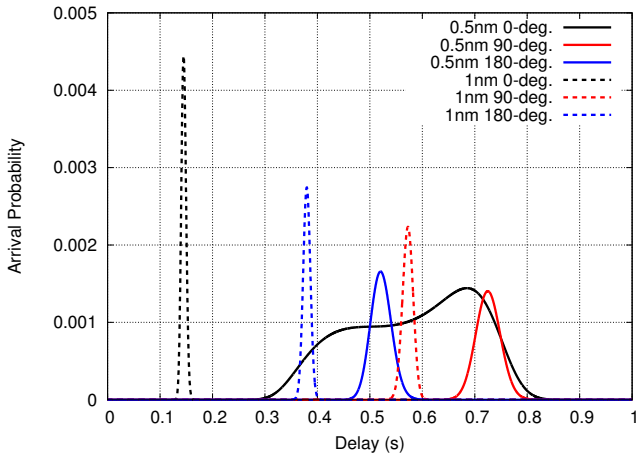

Fig. 4. CIR (delay profile) $\bar{c}(t)/N_{\rm tx}$ at communication distance of $x_0 = 300\,\mu$m for particle sizes $R = \{0.5, 1.0\}$ nm with initial phase $\beta \in \{0, \pi/2, \pi\}$.

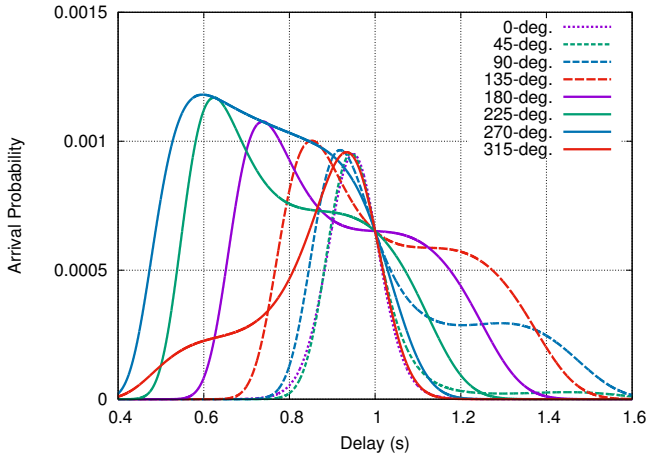

Fig. 5. Impact of phase β on CIR (delay profile) $\bar{c}(t)/N_{\rm tx}$ at communication distance of $x_0 = 300\,\mu$m for particle size $R = 0.3$ nm.

a radius of $R_{\rm rx} = 45$ nm is located $x_0 = 300\,\mu$m apart from the Tx nanomachine.

A. Equalization Algorithm

Due to the intrinsic randomness of diffusion, the Rx nanomachine tries to estimate the expected CIR $\lambda_l[k]$ as discussed in [33], where training sequence designs and practical channel estimation methods achieving near Cramer–Rao bound were investigated. In order to simplify the problem, we assume a perfect knowledge of expected CIR $\boldsymbol{\lambda}[k] \triangleq \big[\lambda_0[k], \lambda_1[k], \ldots, \lambda_L[k]\big]^{\rm T}$, while in practice we should first estimate it by employing such channel estimation methods. Given expected CIR $\boldsymbol{\lambda}[k]$, the Rx nanomachine equalizes the ISI channels. We use an optimal equalizer based on MLSD with a modified Viterbi algorithm proposed in [34].

As discussed in [34], in order to handle long memory of diffusive molecular channels (i.e., theoretically $L = \infty$ due to Gaussian profile), MLSD in practice uses delayed decision-feedback sequence estimation (DDFSE), which is prudent to include the impact of all prior ISI symbols on the current candidate states, whereas only a finite number of trellis states are considered. Let $L' \leq L$ be the explicit channel memory, and thus there will be $2^{L'}$ trellis states in DDFSE, where each state represents a candidate sequence for the previous L' bits for OOK symbols. For a trellis branch corresponding to a candidate sequence $\tilde{\boldsymbol{s}}[k] = \big[1, \tilde{s}[k], \tilde{s}[k-1], \ldots, \tilde{s}[k-L+1]\big]^{\rm T}$, a log-likelihood for the branch in the Viterbi algorithm is given for Poisson channels in (12) as follows:

$$\Phi(\tilde{\boldsymbol{s}}[k]) = -\boldsymbol{\lambda}^{\rm T}\tilde{\boldsymbol{s}}[k] + r[k]\ln(\boldsymbol{\lambda}^{\rm T}\tilde{\boldsymbol{s}}[k]) - \sum_{j=1}^{r[k]}\ln(j), \quad (13)$$

considering the fact that the sum of Poisson RVs is also a Poisson RV, i.e., $r[k] \sim \mathsf{Pois}(\boldsymbol{\lambda}^{\rm T}\boldsymbol{s}[k])$, whose PDF is expressed as $\exp(\Phi(\boldsymbol{s}[k]))$. Note that the candidate sequence $\tilde{\boldsymbol{s}}[k]$ consists of a new branch $\tilde{s}[k]$ for the present bit $s[k]$, current state $\big[\tilde{s}[k-1], \tilde{s}[k-2], \ldots, \tilde{s}[k-L']\big]$, and delayed decisions $\big[\tilde{s}[k-L'-1], \ldots, \tilde{s}[k-L+1]\big]$ for past bits across trellis diagram. The MLSD can be readily generalized to a fractionally-spaced equalization by taking a sum of over-sampled log-likelihoods as studied in [34], where higher over-sampling factor M offers a significant gain if the arrival events of molecules are mutually independent across samples.

The bit-error rate (BER) performance can be analyzed using classical techniques by considering all possible erroneous paths over the trellis diagram. For example, the conditional probability that a true path $\boldsymbol{s}[k]$ will be wrong to an erroneous path $\boldsymbol{s}'[k] \triangleq \boldsymbol{s}[k] + \boldsymbol{\delta}[k]$ is given as follows:

$$\begin{aligned}\Pr(\boldsymbol{s}[k] \to \boldsymbol{s}'[k]) &= \Pr\big(\Phi(\boldsymbol{s}[k]) < \Phi(\boldsymbol{s}'[k])\big) \\ &= \Pr\Big(r[k]\ln\big(1 + \tfrac{\boldsymbol{\lambda}^{\rm T}\boldsymbol{\delta}[k]}{\boldsymbol{\lambda}^{\rm T}\boldsymbol{s}[k]}\big) > \boldsymbol{\lambda}^{\rm T}\boldsymbol{\delta}[k]\Big).\end{aligned} \quad (14)$$

This can be readily calculated by the cumulative distribution function (CDF) of Poisson RV $r[k]$, i.e., $\Pr(r < x) = \Gamma(\lfloor x+1\rfloor, \lambda)/\Gamma(\lfloor x+1\rfloor, 0)$ for $r \sim \mathsf{Pois}(\lambda)$ where $\lfloor\cdot\rfloor$ is the floor function and $\Gamma(x, a)$ denotes the incomplete gamma function:

$$\Gamma(x, a) = \int_a^\infty t^{x-1}\exp(-t){\rm d}t. \quad (15)$$

By taking a product of the error probabilities for the two branch metrics across all possible error transitions, we can analytically obtain the BER of MLSD. It should be noted that the false negative error ($s[k] = 1$ has been wrong) occurs generally more often than false positive error ($s[k] = 0$ has been wrong) due to the non-negativity of Poisson RV. It suggests that it is better to use a non-equiprobable data sequence in order to improve the reliability. In this paper, we consider equiprobable OOK signaling for simplicity.

B. Release Timing and Particle Size Design

As depicted in Figs. 4 and 5, the CIR highly depends on the molecule release timing against the periodic force phase β in addition to the particle size R. It is known that the equalization usually performs better in longer-memory ISI for

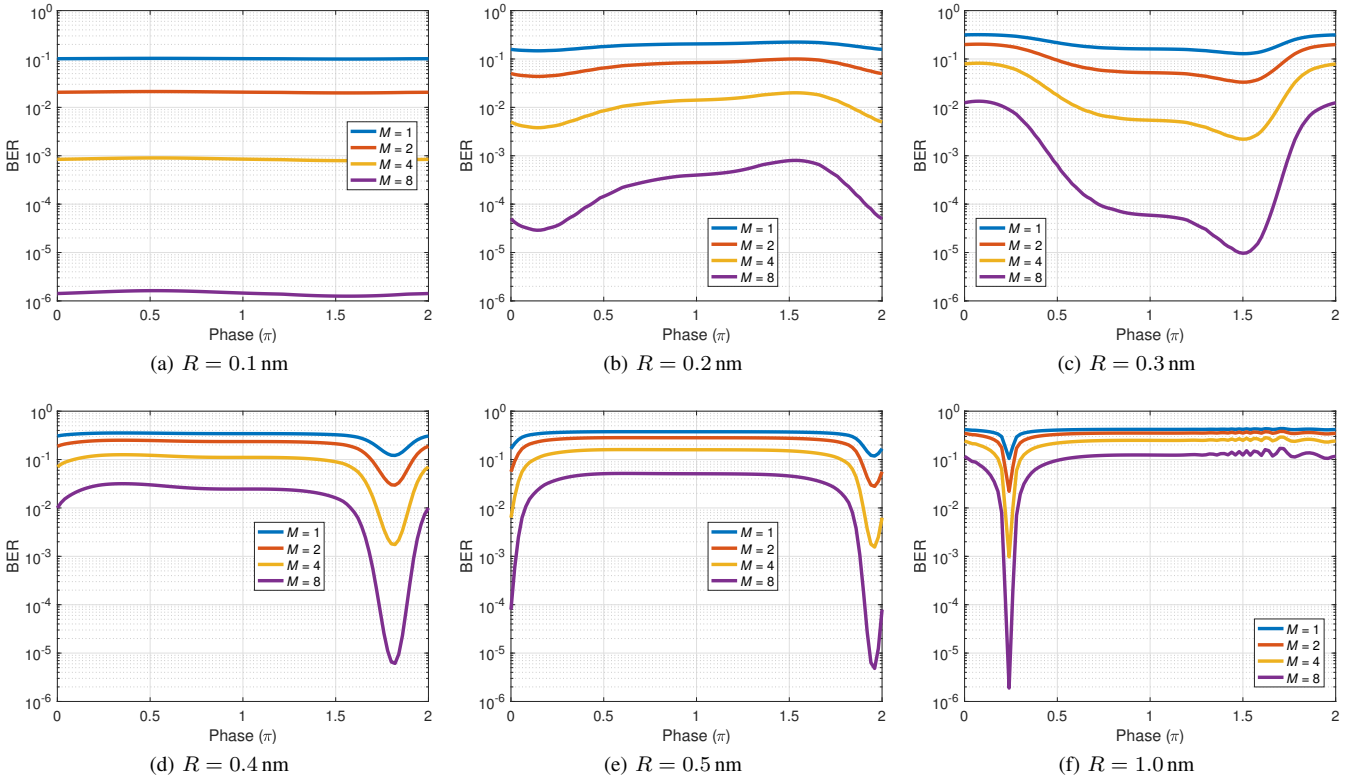

(a) $R = 0.1\,\text{nm}$ (b) $R = 0.2\,\text{nm}$ (c) $R = 0.3\,\text{nm}$

(d) $R = 0.4\,\text{nm}$ (e) $R = 0.5\,\text{nm}$ (f) $R = 1.0\,\text{nm}$

Fig. 6. BER performance as a function of $N_{\text{tx}} = 300$ molecules release timing at sinusoidal force phase β with M-over-sampled fractionally-spaced MLSD for particle sizes $R = \{0.1, 0.2, 0.3, 0.4, 0.5, 1.0\}$ nm, average noise molecules $\lambda_0 = 10$, and communication distance $x_0 = 300\,\mu$m.

wireless fading channels because higher gain due to multi-path diversity can be achieved. In this paper, we show the equalization performance can be also improved in molecular communication channels by considering molecule release timing and particle sizes. In Fig. 6, we plot the BER performance as a function of release timing at force phase β for MLSD employing fractionally-spaced M over-samples. Here, we consider particle sizes of $R \in \{0.1, 0.2, 0.3, 0.4, 0.5, 1.0\}$ nm, and the number of released molecules $N_{\text{tx}} = 300$ with an average number of noise molecules $\lambda_0 = 10$.

As discussed in [34], we can observe that higher over-sampling factor M improves the BER performance more significantly. Because smaller particles have larger diffusion coefficient causing longer memory in general, the BER is relatively less sensitive to the release timing. Nevertheless, it can be seen that the BER performance can vary by several orders of magnitude depending on the release timing for $R \geq 0.2\,\text{nm}$. For example, the best release timing was around $\beta \simeq 1.5\pi$ (i.e, $270\,^\circ$) for a particle size of $R = 0.3\,\text{nm}$ because a longer channel memory appears at this phase as shown in Fig. 5. For larger particle sizes, the performance selectivity is more significant; specifically, the BER performance is extremely poor among most of the release timing except at around $\beta \simeq 0$ for $R = 0.5\,\text{nm}$. It is also because the CIR has longer delay profile at $\beta = 0$ compared to other phases as shown in Fig. 4. In addition, we should notice that the best timing is not always at the time of $\beta = 0$ in which the flow force $F(t)$ is maximal; more specifically, $\beta \simeq 0.24\pi$ was best for $R = 1.0\,\text{nm}$ as shown in Fig. 6(f). Although the smallest particle size of $0.1\,\text{nm}$ in Fig. 6(a) performs the best, using such small particles in the system is often unrealistic. Therefore, it is suggested that we shall design the communications system to fully utilize the knowledge of fluid environment, e.g., by optimizing the timing of molecule release and particle size, such that the CIR memory can be sufficiently large to enjoy the diversity gain.

C. Adaptive Molecule Loading

The BER performance is also dependent on the number of released molecules N_{tx}. In general, the release of more molecules provides more reliable data transmission, as shown in Fig. 7, where we plot BER vs. phase β with a different number of molecules of $N_{\text{tx}} \in \{100, 200, \ldots, 600\}$ for a particle size of $R = 0.3\,\text{nm}$ and an over-sampling factor of $M = 8$ for MLSD. However, the Tx nanomachine may have a physical limitation on the maximum number of molecules transferable in a certain time period. If the system has no ability to use adaptive bit loading with higher-order modulation such as 4-ary pulse-amplitude modulation (PAM) rather than OOK, one possible way to efficiently utilize the finite number of molecules is the aforementioned timing control, where all available molecules are released at around the best phase achieving the lowest BER. However, such a selective time resource allocation may constrain the total throughput.

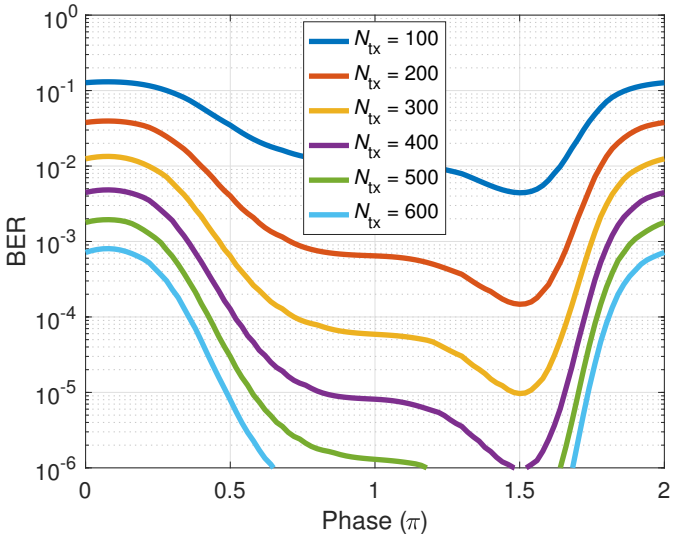

Fig. 7. Impact of the number of releasing molecules $N_{\mathrm{tx}} \in \{100, 200, \ldots, 600\}$ for $R = 0.3\,\mathrm{nm}$ and $M = 8$ over-sampling.

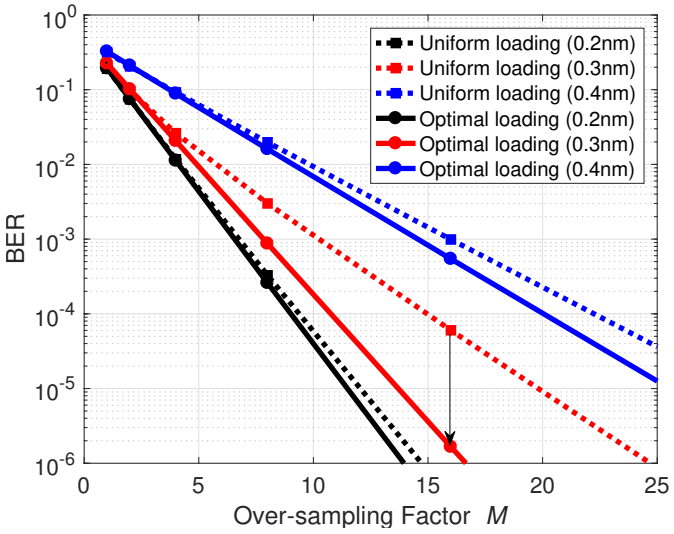

Fig. 8. Impact of adaptive molecule loading N_{tx} to flatten BER over flow cycle for $R \in \{0.2, 0.3, 0.4\}$ nm.

As an alternative way for efficient time resource allocation, we consider an adaptive molecule loading, which saves the number of molecules at good timing and uses more molecules at bad timing to flatten the BER performance across the whole time.

In order to optimize the number of molecules adaptive to the cyclic force, we consider a few discrete phases β and molecule loading N_{tx} to minimize the worst BER subject to a condition that average number of molecules over cycle T remains constant of $\bar{N}_{\mathrm{tx}} = 300$. We divide the cycle into B regions, bth of which is $\beta[b] \in \big[2\pi(b-1)/B, 2\pi b/B\big)$ for $b \in \{1, 2, \ldots, B\}$. The granularity of controllable number of releasing molecules is assumed to be 50, and thus $N_{\mathrm{tx}} \in \{50, 100, 150, \ldots\}$ is assigned to each region depending on the reliability. The following discrete optimization was carried out:

$$\min_{\{N_b\}} \quad \frac{1}{B}\sum_{b=1}^{B} \mathsf{BER}_b(N_b), \quad \text{s.t} \quad \frac{1}{B}\sum_{b=1}^{B} N_b \le \bar{N}_{\mathrm{tx}}, \qquad (16)$$

where $\mathsf{BER}_b(n)$ denotes an average BER within the bth region provided that $N_{\mathrm{tx}} = n$ molecules are used. This adaptation may need a prior knowledge of communication distance, particle size, flow dynamics, and so on.

Fig. 8 shows the BER averaged over the whole cycle as a function of over-sampling factor M to show the benefit of adaptive molecule loading. It is demonstrated in this figure that optimal molecule loading can offer a significant performance improvement. For example, average BER performance for a particle size of $R = 0.3\,\mathrm{nm}$ can be improved by more than one order of magnitude at an over-sampling factor of $M = 16$, with an adaptive molecule loading. Although the adaptive loading requires complicated control compared to oversampling, such a significant gain in BER performance is remarkable for molecular communications.

IV. Conclusions

We investigated molecular communications in drift-diffusion fluid environment where periodic flow force is present, motivated by the fact that biological functionality is often cyclic, e.g., heart pumping. We made an analysis of cyclic CIR in such an environment. It is found that the channel memory highly depends on the molecule release timing and particle size. Through the analysis, we showed a potential performance improvement by designing release timing and sizes for molecular communications. By exploiting the multi-path diversity with channel equalization, it was verified that the BER performance can be improved by several orders of magnitude if we intentionally release the molecules at the timing when the CIR memory can be long enough. Further rigorous analyses under more realistic environments such as non-sinusoidal flow, low-complexity equalizers, and high-order modulation schemes remain as future works.

References

[1] A. Goeland and V. Vogel, "Harnessing biological motors to engineer systems for nanoscale transport and assembly," *Nat. Nanotechnol.*, vol. 3, pp. 465–475, 2008.

[2] P. E. M. Purnick and R. Weiss, "The second wave of synthetic biology from modules to systems," *Nat. Rev. Mol. Cell Bio.*, vol. 10, no. 6, pp. 410–422, 2009.

[3] R. A. Freitas, "Current status of nanomedicine and medical nanorobotics," *J. Computational and Theoretical Nanoscience*, vol. 2, no. 1, pp. 1–25, 2005.

[4] T. Suda, M. Moore, T. Nakano, R. Egashira, and A. Enomoto, "Exploratory research on molecular communication between nanomachines," *ACM Genetic and Evol. Computat. Conf.*, 2005.

[5] T. Nakano, A. Eckford, and T. Haraguchi, *Molecular Communication*, Cambridge University Press, 2013.

[6] T. Nakano, M. Moore, F. Wei, A. V. Vasilakos, and J. W. Shuai, "Molecular communication and networking: Opportunities and challenges," *IEEE Trans. NanoBiosci.*, vol. 11, no. 2, pp. 135-148, 2012.

[7] I. Akyildiz, F. Brunetti, and C. Blazquez, "Nanonetworks: A new communication paradigm," *Comput. Netw.*, vol. 52, 2008.

[8] Y. Moritani, S. Hiyama, and T. Suda, "Molecular communication for health care applications," *IEEE Int. Conf. Pervasive Comput. Commun. Workshops*, 2006.

[9] J. Suzuki, D. H. Phan, and H. Budiman, "A nonparametric stochastic optimizer for TDMA-based neuronal signaling," *IEEE Trans. NanoBioscience*, vol. 13, no. 3, pp. 244–254, 2014.

[10] M. Pierobon and I. F. Akyildiz, "Diffusion-based noise analysis for molecular communication in nanonetworks," *IEEE Trans. SP*, vol. 59, no. 6, 2011.

[11] K. V. Srinivas, R. S. Adve, and A. W. Eckford, "Molecular communication in fluid media: The additive inverse Gaussian noise channel," *IEEE Trans. IT*, vol. 58, no. 7, 2012.

[12] N. Farsad, A. Eckford, S. Hiyama, and Y. Moritani, "A simple mathematical model for information rate of active transport molecular communication," *IEEE INFOCOM*, 2011.

[13] M. J. Moore and T. Suda, "Molecular communication: Modeling noise effects on information rate," *IEEE Trans. NanoBiosci.*, vol. 8, no. 2, 2009.

[14] J. S. Mitzman, B. Morgan, T. M. Soro, J. Suzuki, and T. Nakano, "A feedback-based molecular communication protocol for noisy intrabody environments," *IEEE Int. Conf. E-health Networking Applications and Services*, 2015.

[15] T. Nakano, Y. Okaie, and A. V. Vasilakos, "Transmission rate control for molecular communication among biological nanomachines," *IEEE JSAC*, vol. 31, no. 12, pp. 835-846, 2013.

[16] L. Felicetti, M. Femminella, G. Reali, T. Nakano, and A. V. Vasilakos, "TCP-like molecular communications," *IEEE JSAC*, vol. 32, no. 12, pp. 2354-2367, 2014.

[17] X. Wang, M. D. Higgins, and M. S. Leeson, "Simulating the performance of SW-ARQ schemes within molecular communications," *Simulation Modelling Practice and Theory*, vol. 42, 2014.

[18] C. Bai, M. S. Leeson, and M. D. Higgins, "Performance of SW-ARQ in bacterial quorum communications," *Nano Commun. Netw.*, vol. 6, no. 1, 2015.

[19] M. S. Leeson and M. D. Higgins, "Forward error correction for molecular communications," *Nano Commun. Netws*, vol. 3, no. 3, pp. 161-167, 2012.

[20] —, "Error correction coding for molecular communications," *IEEE ICC*, pp. 6172-6176, 2012.

[21] Y. Lu, M. D. Higgins, and M. S. Leeson, "Self-orthogonal convolutional codes (soccs) for diffusion-based molecular communication systems," *IEEE ICC*, pp. 1049-1053, 2015.

[22] C. Bai, M. S. Leeson, and M. D. Higgins, "Minimum energy channel codes for molecular communications," *Electron. Lett.*, vol. 50, no. 23, pp. 1669-1671, 2014.

[23] H. Egashira, J. Suzuki, J. S. Mitzman, T. Nakano, and H. Fukuda, "Robust directional-diffusive hybrid molecular communication with parity-check erasure coding," *IFSA-SCIS*, 2017.

[24] A. Noel, K. Cheung, and R. Schober, "A unifying model for external noise sources and ISI in diffusive molecular communication," *IEEE JSAC*, vol. 32, no. 12, pp. 2330-2343, Dec. 2014.

[25] M. Pierobon and I. Akyildiz, "A physical end-to-end model for molecular communication in nanonetworks," *IEEE JSAC*, vol. 28, no. 4, pp. 602-611, May 2010.

[26] D. Miorandi, "A stochastic model for molecular communications," *Nano Commun. Netw.*, vol. 2, no. 4, pp. 205-212, 2011.

[27] G. Wei and R. Marculescu, "Miniature devices in the wild: Modeling molecular communication in complex extracellular spaces," *IEEE JSAC*, vol. 32, no. 12, pp. 2344-2353, Dec. 2014.

[28] N. Farsad, A. Eckford, and S. Hiyama, "A Markov chain channel model for active transport molecular communication," *IEEE Trans. SP*, vol. 62, no. 9, pp. 2424-2436, May 2014.

[29] A. Bicen and I. Akyildiz, "End-to-end propagation noise and memory analysis for molecular communication over microfluidic channels," *IEEE Trans. Commun.*, vol. 62, no. 7, pp. 2432-2443, July 2014.

[30] A. Akkaya, H. Yilmaz, C.-B. Chae, and T. Tugcu, "Effect of receptor density and size on signal reception in molecular communication via diffusion with an absorbing receiver," *IEEE Commun. Lett.*, vol. 19, no. 2, pp. 155-158, Feb. 2015.

[31] M. Moore, T. Nakano, A. Enomoto, and T. Suda, "Measuring distance from single spike feedback signals in molecular communication," *IEEE Trans. SP*, vol. 60, no. 7, pp. 3576-3587, July 2012.

[32] A. Noel, K. Cheung, and R. Schober, "Bounds on distance estimation via diffusive molecular communication," *IEEE GLOBECOM*, pp. 2813-2819, Dec. 2014.

[33] V. Jamali, A. Ahmadzadeh, C. Jardin, H. Sticht, and R. Schober, "Channel estimation techniques for diffusion-based molecular communications," *IEEE ICC*, 2015.

[34] A. Noel, K. Cheung, and R. Schober, "Optimal receiver design for diffusive molecular communication with flow and additive noise," *IEEE Trans. NanoBiosci.*, vol. 13, no. 3, pp. 350-362, Sept. 2014.

[35] M. Mahfuz, D. Makrakis, and H. Mouftah, "A comprehensive study of sampling-based optimum signal detection in concentration-encoded molecular communication," *IEEE Trans. NanoBiosci.*, vol. 13, no. 3, pp. 208-222, Sept. 2014.

[36] A. Ahmadzadeh, A. Noel, A. Burkovski, and R. Schober, "Amplify-and-forward relaying in two-hop diffusion-based molecular communication networks," *IEEE GLOBECOM*, 2015.

[37] A. Noel, K. C. Cheung, and R. Schober, "Using dimensional analysis to assess scalability and accuracy in molecular communication," *IEEE ICC MONACOM*, Jun. 2013.

[38] D. W. Holdsworth, C. J. D. Norley, R. Frayne, D. A. Steinman, and B. K. Rutt, "Characterization of common carotid artery blood-flow waveforms in normal human subjects," *Physiol. Meas.*, vol. 20, no. 3, pp. 219–240, Aug. 1999.

[39] P. Nelson, *Biological Physics: Energy, Information, Life*, W. H. Freeman and Company, 2008.

[40] H. Arjmandi, A. Gohari, M. Kenari, and F. Bateni, "Diffusion-based nanonetworking: A new modulation technique and performance analysis," *IEEE Commun. Lett.*, vol. 17, no. 4, pp. 645-648, Apr. 2013.

[41] C. Gardiner, *Stochastic Methods*, Springer Series in Synergetics (Springer-Verlag, Berlin, 2009). 1985.